JOURNAL OF GEOPHYSICAL RESEARCH, VOL. 105, NO. A10, PAGES 22,943–22,953, OCTOBER 1, 2000

Variation of mesospheric ozone during the highly relativistic electron event in May 1992 as measured by the High Resolution Doppler Imager instrument on UARS

W. Dean Pesnell,[1] Richard A. Goldberg,[2] Charles H. Jackman,[3] D. L. Chenette,[4] and E. E. Gaines[4]

Abstract. Highly relativistic electron precipitation events (HREs) include long-lived enhancements of the flux of electrons with $E > 1$ MeV into the Earth's atmosphere. HREs also contain increased fluxes of electrons with energies above 100 keV that have been predicted to cause large depletions of mesospheric ozone. For some of the measured instantaneous values of the electron fluxes during the HRE of May 1992, relative depletions greater than 22% were predicted to occur between altitudes of 55 and 80 km, where HO_x reactions cause local minima in both the ozone number density and mixing ratio altitude profiles. These ozone depletions should follow the horizontal distribution of the electron precipitation, having a distinct boundary equatorward of the $L = 3$ magnetic shell. To search for these effects, we have analyzed ozone data from the High Resolution Doppler Imager (HRDI) instrument on UARS. Owing to the multiple, off-track viewing angles of HRDI, observations in the region affected by the electrons are taken at similar local solar times before, during, and after the electron flux increase. Our analysis limits the relative ozone depletion to values $< 10\%$ during the very intense May 1992 HRE. We do observe decreases in the ozone mixing ratio at several points in the diurnal cycle that may be associated with the transport of water vapor into the mesosphere during May 1992. This masking of the precipitating electron effects by the seasonal variations in water vapor can complicate the detection of those effects.

1. Introduction

Ozone is one of the most studied molecules in the Earth's atmosphere. Much of this research has involved the stratosphere, where man-made compounds destroy ozone in the southern polar regions during the austral spring (for a summary, see *Bojkov* [1995]). As a result of the long-term ozone database developed by this research, solar proton events are now known to modulate stratospheric ozone [e.g., *Thomas et al.*, 1983; *McPeters and Jackman*, 1985]. Energetic electrons are also modulated by solar activity, but even the most energetic can penetrate only to the mesosphere and upper stratosphere before depositing their energy [*Thorne*, 1977; *Baker et al.*, 1993]. As a result, relativistic electron precipitation events (REPs) were considered a possible source for ionization-induced chemical changes in the stratosphere and mesosphere [*Thorne*, 1977]. We describe here an attempt to detect these effects during what we consider an optimum energetic electron event, the highly relativistic electron event of May 1992.

Satellite measurements show large enhancements of the electron flux at relativistic energies ($E > 1$ MeV) throughout the inner magnetosphere during geomagnetic storms. Initially, the injected electrons fill the entire pitch angle range, but those within the bounce loss cone rapidly precipitate into the atmosphere so that the evolution of the system becomes dominated by the slower process of pitch angle diffusion. Stably trapped electrons are scattered into the loss cone by magnetospheric waves via an energy-dependent process that takes from several days to months to remove the electrons. The most significant and longest lasting precipitating fluxes measured by the particle environment monitor (PEM) high-energy particle spectrometer (HEPS) instrument on the Upper Atmosphere Research Satellite (UARS) are observed to be in the range of magnetic L shell parameter $3 < L \leq 4$. (For a magnetic coordinate we are using the McIlwain L shell, where $L = 1/\cos^2(\Lambda)$ and Λ is the invariant latitude.) These enhanced electron fluxes at relativistic energies are termed highly relativistic electron events (HREs).

[1]Nomad Research, Inc., Bowie, Maryland.

[2]Laboratory for Extraterrestrial Physics, NASA Goddard Space Flight Center, Greenbelt, Maryland.

[3]Laboratory for Atmospheres, NASA Goddard Space Flight Center, Greenbelt, Maryland.

[4]Space Physics Department, Lockheed Martin Advanced Technology Division, Palo Alto, California.

Paper number 2000JA000091.
0148-0227/00/2000JA000091$09.00

Based on satellite data observed at geosynchronous orbit, HREs are most pronounced during the declining phase of the solar cycle, increasing in intensity, spectral hardness, and frequency of occurrence as the solar cycle reaches minimum [*Baker et al.*, 1979, 1986, 1987, 1993; *Rostoker et al.*, 1998]. From comparisons with lower-altitude satellites [*Imhof et al.*, 1991], and from our rocket study of a modest HRE [*Herrero et al.*, 1991; *Baker et al.*, 1993], it is apparent that a significant fraction of the outer zone electrons associated with an HRE will eventually reach the middle atmosphere, where they can strongly influence the electrodynamics and composition (e.g., O_3 and OH) of that region [*Goldberg et al.*, 1995a,b]. As the drift period of electrons with $E > 0.1$ MeV is less than 1 hour [*Walt*, 1994], these electrons average over the diurnal variation of the terrestrial magnetic field and have a roughly symmetric distribution in magnetic longitude at a constant value of L [*Vampola and Gorney*, 1983]. Since HREs can sustain their activity for several weeks, recur over several solar rotations, and cover a more extensive region in longitude and latitude than does the auroral zone, their impact on the middle atmosphere could be large. If the cumulative effect of HREs on the high-latitude mesosphere is a significant source of chemical rearrangement, they should be included in any consideration of the long-term evolution of the mesosphere.

A decrease in ozone near and above the stratopause was observed by the Aurorozone 1 rocket and attributed to the chemical effects of the combined X-ray and REP-induced ionization [*Goldberg*, 1979]. Effects of the precipitation of energetic magnetospheric electrons on the mesosphere were also studied with radio propagation [*Lauter and Knuth*, 1967; *Potemra and Zmuda*, 1970; *Spjeldvik and Thorne*, 1975], recognizing that the enhanced ionization produced by the incoming electrons scatters and attenuates radio waves. Many of these radio propagation studies extrapolated electron flux energy spectra to relativistic energies with a power law and noted that the large ionization that would result in the mesosphere fit their observations. We will show that the electron fluxes with $E > 1$ MeV do not follow the time dependence of the lower-energy fluxes and must be derived from in situ measurements of the flux at and above 1 MeV.

Referring to Figure 1, where the penetration altitude of vertically incident electrons is shown as a function of energy, we see that electrons with $E \geq 100$ keV will produce ions that can then create HO_x radicals between altitudes of about 60 and 80 km that could affect the ozone balance in that region. When measured instantaneous electron fluxes are used in both steady state and time-dependent photochemical models, ozone depletions up to 22% are predicted at mesospheric altitudes (see section 3 below and *Baker et al.* [1986], *Goldberg et al.* [1994, 1995a,b], and *Aikin and Smith* [1999]). The predicted relative depletion in ozone peaks between altitudes of 65 and 75 km, where HO_x reactions cause a local minimum in the altitude profile of the ozone number density [*Pesnell et al.*, 1999; *Fleming et al.*, 1995]. We have searched for those predicted ozone depletions in ozone data from the High Resolution Doppler Imager (HRDI) on UARS, whose altitude coverage spans the region of the minimum.

Individual measurements of ozone could sample a region depleted of ozone by a recent or ongoing burst of electrons. Although the ozone data hve considerable noise, a depletion of 20% should be observable in the HRDI ozone data. We have also considered the effect of the more conservative

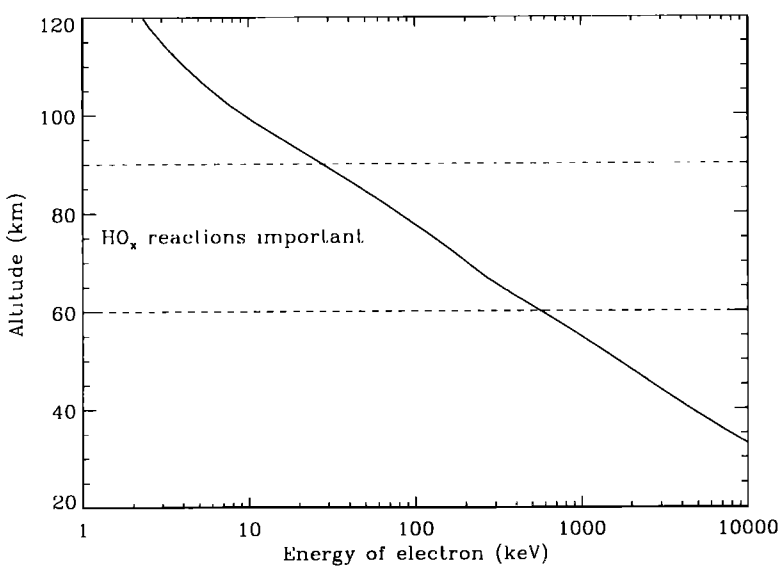

Figure 1. Penetration altitude of vertically incident electrons in the terrestrial atmosphere, as determined from the range of electrons in an atmospheric model. A dotted vertical line is drawn at an electron energy of 1 MeV to show how deep an HRE can reach. The region where HO_x reactions dominate the determination of the ozone concentration is marked by dashed lines. Below 60 km altitude other catalytic reagents, such as NO_x and halogenous molecules, become as important as HO_x in determining the ozone concentration. Above 90 km altitude the ozone concentration is determined by the Chapman cycle.

daily-averaged electron fluxes, which should be a reliable indicator of the daily ion generation in the mesosphere by the HRE. Ozone depletions of $< 8\%$ are predicted when these fluxes are used in the ion production calculations. When HRDI data from May 1992 are displayed against local solar time (LST), the depletions should be seen by comparing ozone measurements made at similar values of LST but observed either before and during the HRE or during and after the HRE. Average values over 30 min LST bins were used to try to extract the anticipated depletion signal. Results of this analysis are reported here.

We shall discuss first the variation of the energy input into the mesosphere due to energetic electrons as measured by PEM HEPS. Next, we shall discuss our expectations of how that input would change the ozone in the mesosphere, the HRDI measurements that test these expectations, and how changes in water vapor content could influence the ozone measurements.

2. UARS Particle Measurements From PEM

The PEM HEPS instruments on UARS provide pitch-angle- and energy-resolved measurements of the low-altitude electron flux between 30 keV and 5 MeV [*Winningham et al.*, 1993]. For the present analysis the pitch angle resolution in the measurements is used to distinguish those electron fluxes which are stably trapped (i.e., they have estimated mirror altitudes above 100 km) from those in the bounce loss cone (BLC). The latter will directly precipitate into the atmosphere.

Estimates of the precipitating electron flux were derived from the HEPS measurements by counting BLC flux measurements only when the full angular range of a sensor is within the BLC. If the loss cone is filled by small-angle scattering, this procedure tends to underestimate the total precipitating flux because it is biased against measurements at the edge of the BLC, where that flux would be more intense [*Imhof and Gaines*, 1993]. Therefore the estimated decreases in ozone due to these electrons are lower limits; larger decreases would not necessarily have been inconsistent with these predictions.

The direct measurement of the precipitating electron flux at low altitude provided by HEPS is more reliable than estimates based on measurements from, for example, geosynchronous satellites, or by scaling total electron flux measurements. As shown by *Gaines et al.* [1995], temporal variations in the electron flux intensity and their energy distributions can vary significantly between the trapped and precipitating components. In particular, the trapped flux is seen to last longer than the precipitating flux. We will show some of the differences for the period October 1991 through November 1993. In this paper, daily averages of the electron fluxes within L shells are used to illustrate the electron input. Although such a procedure tends to average out small-scale variations in space or time, the short drift periods of the energetic electrons considered here tend to spread the electron flux along the L shells. This reduces the effects of the diurnal variations in the magnetic field on the flux amplitude [*Vampola and Gorney*, 1983]. Hemispheric variations, where fluxes in the Southern Hemisphere are typically larger than in the Northern Hemisphere, are also averaged out in this analysis. We believe that this is most appropriate for our study, recognizing that locally and on small scales, larger chemical effects might be observed.

As we now show, the highly relativistic electron fluxes of May 1992 were the most intense, most energetic, and longest lived of the HREs seen by UARS in the first two years of the UARS mission. Within the belt of magnetic L shell $3 < L \leq 4$ (or invariant latitudes between 55° and 60°), the locally precipitating flux of electrons with $E > 100$ keV and $E > 1$ MeV reached a large value on May 11 and continued at this value until May 21 (see the stippled feature of Figure 2a and the discussion in *Gaines et al.* [1995]). It then decreased

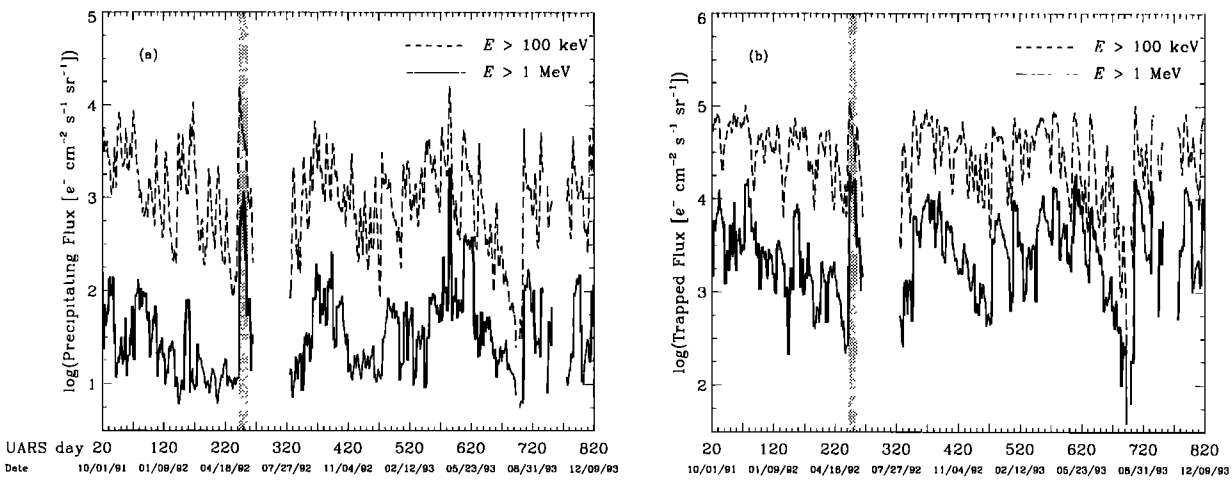

Figure 2. (a) Fluxes of precipitating electrons (in units of electrons cm^{-2} s^{-1} sr^{-1}, and we show the common log of the flux) with $E > 1$ MeV and $E > 100$ keV during the prime mission period of UARS (October 1, 1991 through December 9, 1993). A 3 day running average was used to reduce to day-to-day fluctuations of the data. The May 1992 HRE is stippled. (b) The trapped electron flux for a similar period of time.

by a factor of about 8 in magnitude and continued through May 27. Compared to background effects for magnetically undisturbed times and locations, the ion production rate in the lower mesosphere due to electrons increased by at least a factor of 100 during this HRE. For comparison, the trapped fluxes for the same energy bands are shown in Figure 2b. A good example of how the trapped flux time dependence differs from the precipitating flux can be seen by comparing the $E > 1$ MeV fluxes between UARS days 370 and 470. The trapped flux continues decaying throughout this time, while the precipitating flux has dropped to a low value by UARS day 420. During the same time period the trapped flux with $E > 100$ keV has a small decay while the precipitating flux with $E > 100$ keV drops an order of magnitude.

3. Predicted Loss of Ozone Due to Electron Precipitation

From the measured precipitating electron energy spectra, we have derived the energy deposition height profiles using techniques of *Goldberg et al.* [1984]. For May 18, 1992, Figure 3 shows the ion pair production rate (Q) profiles for two bands of $L = \bar{L} \pm 1/8$ and for one large burst. We found that the zone of maximum energy deposition was centered about $L = 3.75$. From these profiles it is apparent that even for the day-averaged electron fluxes, large quantities of ions are produced down to 50 km, far deeper than produced during other kinds of electron precipitation events. As another example, evidence of an ionospheric C region near an altitude of 50 km was found during an HRE in 1990 [*Goldberg et al.*, 1994].

Once Q was calculated from the HEPS electron flux observations, we used two models to calculate the predicted relative change in mesospheric ozone. First, the Goddard Space Flight Center 2D chemistry and transport model (see, for example, *Jackman et al.* [1996]) was used to study the average influence of HREs on mesospheric ozone. This model was used to study charged particle effects on stratospheric ozone from solar proton events [*Jackman*, 1991; *Jackman et al.*, 1990, 1996] and ozone in the upper stratosphere and lower mesosphere during several HREs [*Pesnell et al.*, 1999; *Goldberg et al.*, 1995a]. The model computes daytime averaged values rather than following the diurnal cycles of constituents. The results of the model are thus most appropriate for long-term particle precipitation events, such as the May 1992 HRE, that last from days to weeks. Another model, which computes the ion-neutral chemistry through the diurnal cycle, was used to understand the LST-dependent effects of the electron-produced ions on the HO_x chemistry [*Aikin and Smith*, 1999]. During an HRE, their model shows that high-latitude mesospheric ozone will be reduced for values of LST between sunrise and local noon, but in the afternoon the sensitivity to the enhanced HO_x concentration is greatly reduced and the ozone concentration is close to its non-HRE value. Thus we should look in the morning hours for a reduction in ozone due to the HRE.

Concentrations of the HO_x constituents vary over the course of the day, driven by their production and loss mechanisms. The background source of HO_x strongly depends on the ambient H_2O concentration and the solar zenith angle (or LST) through the photolysis of H_2O and the reaction of $O(^1D)$ with H_2O. The H_2O in the GSFC-2D model is computed self-consistently and is in reasonable agreement with Halogen Occultation Experiment (HALOE) measurements in the mesosphere [*Chandra et al.*, 1997]. The H_2O concentration in the LST-dependent model was set to the value obtained in the GSFC-2D model as a baseline. Cases were also run with this model using twice and one half the H_2O concentration.

To understand the presentation and analysis of the ozone data, it is necessary to review the diurnal cycle of mesospheric ozone. A simplified chemistry for mesospheric ozone

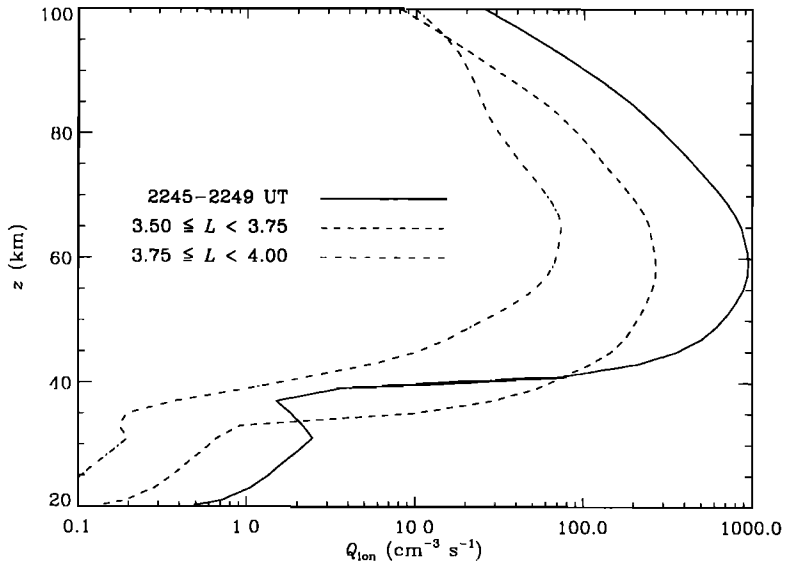

Figure 3. Ion production rates for the day-averaged electron fluxes of May 18, 1992, for two ranges of L and for a large localized precipitating burst of electron flux.

follows only the oxygen compounds as they cycle between O, O_2, and O_3 [*Brasseur and Solomon*, 1986, section 5.2]. In this model, as is also observed in the mesosphere, ozone is the reservoir of odd-oxygen at night. At sunrise, O_3 is destroyed by solar UV radiation, releasing the O that is the daytime reservoir of odd-oxygen. Over the course of the sunlit hours, O and O_3 are produced and destroyed by various reactions, until sunset when the three-body reaction

$$O + O_2 + M \rightarrow O_3 + M \quad (1)$$

again rapidly removes O from the mesosphere. This Chapman cycle model agrees qualitatively with the mesospheric data, but additional reactions are necessary for quantitative agreement.

In the presence of water vapor, a competing set of reactions:

$$H_2O + h\nu \rightarrow H + OH, \quad (2)$$
$$H_2O + O(^1D) \rightarrow 2OH, \quad (3)$$
$$H + O_3 \rightarrow OH + O_2, \quad (4)$$
$$OH + O \rightarrow H + O_2, \quad (5)$$
$$\text{Net: } O_3 + O \rightarrow O_2 + O_2, \quad (6)$$

act to destroy odd-oxygen in the mesosphere and alter the diurnal cycle of ozone in several LSTs [e.g., *Aikin and Smith*, 1999; *Allen et al.*, 1984]. During the night the ozone concentration is reduced compared to the pure oxygen model due to the removal of odd-oxygen by the HO_x reactions in equations (4)–(5). Immediately after the sunrise water vapor is dissociated by solar Lyman α photons (equation [2]) and by excited state $O(^1D)$ created by the photolysis of O_2 and O_3 (equation [3]). At the same time, O produced by photodissociation of O_2 combines with other O_2 to form ozone. At or before local noon, the destruction of O_3 via the HO_x reactions in equations (4)–(5) matches the production, and a local maximum concentration of ozone is reached. As the solar zenith angle then increases and the solar irradiation decreases, the HO_x abundance starts to decrease, but the chemical lifetime of HO_x exceeds that of O and its influence on the odd-oxygen content continues throughout the day. After sunset the O_3 concentration recovers to the nighttime value. Owing to the HO_x reactions, a maximum in the ozone mixing ratio should be present in the morning hours, typically before noon with the normal water vapor content. In the absence of energetic electrons, the location of the maximum ozone concentration is a function of the water vapor concentration, with the maximum in the ozone concentration at a given altitude moving to earlier LST as the water vapor concentration increases [*Aikin and Smith*, 1999].

Ions produced during an HRE can, through complicated ion chemistry, enhance HO_x compounds and influence the ozone concentration during the particle event [*Solomon et al.*, 1981, 1983]. Approximately two HO_x species are produced from each ion pair up to about 70 km. However, above 70 km, the production of HO_x species from each ion pair has a strong dependence on the ionization rate and the duration of the particle precipitation event [*Solomon et al.*, 1981]. Our model calculations use the production of HO_x constituents per ion pair as a function of altitude from Figure 2 of *Solomon et al.* [1981] for moderate ionization rates. This accounts for the rapid dropoff in ion-related HO_x production with altitude above 70 km and is within 5% of their rates for the ion production rates in Figure 3.

We input an assumed continuous sources of HRE-related HO_x production for the ion production rate curves in Figure 3 into both models at 65°N to predict the ozone change. Our simulated ozone percentage change due to the HREs is computed by comparing a model run that includes the electron-induced HO_x compounds with another model run without the HRE flux. Results from the GSFC-2D model are presented in Figure 4. The peak computed ozone decrease due to a burst of HRE precipitation is about 22% at 0.4 mbar ($\sim$70 km), calculated assuming the burst HRE flux continued for several hours. However, as the probability of detecting the response to a burst is quite small, we also include the ozone changes due to the day-averaged fluxes, which should be more easily measured. In particular, we can average ozone measurements to increase the signal-to-noise ratio of the data. The peak computed ozone decrease is now 8% or so, a smaller depletion but one that should be seen if data with sufficient signal-to-noise ratio exist.

4. UARS HRDI Ozone Measurements

The UARS measurements can be used to help quantify the ozone change and determine if the May 1992 HREs could be responsible for a significant ozone variation. HRDI uses a Fabry-Perot interferometer to measure the radiance of an O_2 line which is then used to determine the ozone mixing ratio [*Hays et al.*, 1993; *Burrage et al.*, 1996]. Altitude profiles of HRDI measurements were supplied as 3AT files by the HRDI Science Team at the University of Michigan. Each file contains a day's worth of data sampled at intervals of 65.536 s. Profiles of measured quantities are given on fixed altitude grids, corresponding to a 3 km spacing in the mesosphere. Although quality flags are included in the files, they do not contain error estimates but simply indicate whether or not a data point is included at that altitude. Data from May 1992 with geographic locations within the magnetic L shell band $3 < L \leq 4$ were extracted from the HRDI files and analyzed using algorithms described by *Pesnell et al.* [1999].

UARS has a precessing orbit, requiring roughly 34 days to scan the instruments 12 hours in LST. At the beginning of a yaw cycle, HRDI begins measuring atmospheric parameters at four values of LST, two in the A.M. branch near noon and two in the P.M. branch near midnight. Because HRDI measures scattered sunlight, no data is returned from any branch when the Sun is absent. As the yaw cycle progresses, both branches move to earlier values of LST, reaching near midnight and noon, respectively, just before the turning of the satellite that starts the next yaw cycle. Coverage of the day-lit portion of the diurnal cycle is available for a given latitude band by combining observations of the A.M. and P.M. branches observed over a yaw cycle. The cold side of UARS was pointed north during May 1992, so all of the ozone mea-

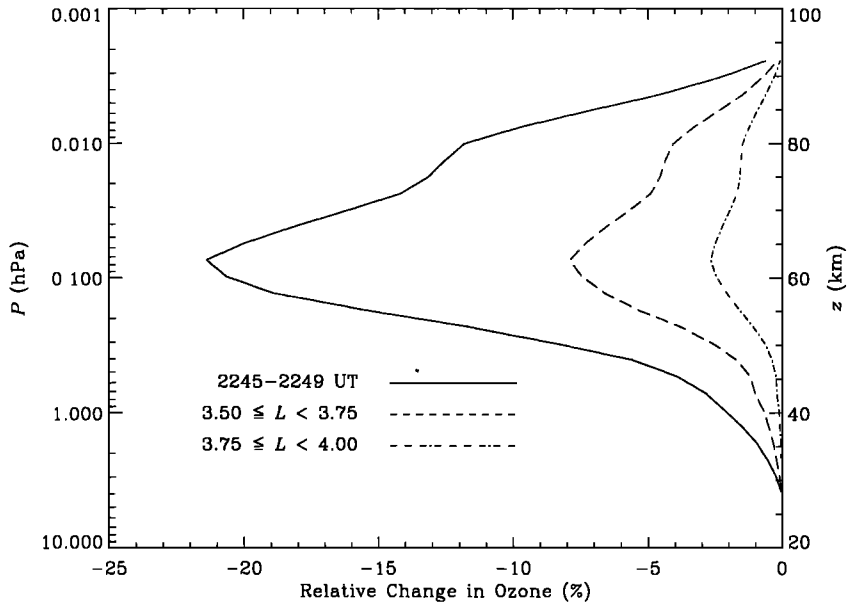

Figure 4. Ozone depletions for May 18, 1992, derived from the ion production rates in Figure 4. Note that all three profiles peak between 60 and 65 km altitude, with substantial depletions occurring at 69 km, the lowest altitude for which HRDI data with complete coverage are available.

surements are in the northern polar region throughout the HRE.

One advantage of the multiple viewing angles of HRDI is the overlapping coverage of the diurnal cycle by measurements made at two different angles to the UARS viewing angle, particularly near noon. This should be compared with the data from cryogenic limb array etalon spectrometer (CLAES) and microwave limb sounder (MLS) on UARS, which sweep out the LST values in a more monotonic fashion through a yaw cycle [*Pesnell et al.*, 1999]. As we show below, there are four bands of LST values where ozone is measured in two of the three conditions: before, during, or after the May 1992 HRE. To understand these data, we show the LST variation at several altitudes and then the altitude variation within the overlapping bands.

5. Local Solar Time Analysis

As the electron fluxes that define an HRE are approximately zonally symmetric in magnetic coordinates, we have examined the behavior of ozone as a function of LST during May 1992 in magnetic coordinates. By plotting the data as a function of LST we ensure that comparisons of ozone are made at similar physical conditions, except for the presence of the HRE flux. Once the rapid changes near sunrise and sunset are omitted, the diurnal variation of ozone is smooth, and an HRE-induced change should be visible when compared to ozone that is not being irradiated. Thus the non-HRE values of ozone are treated as standards to which the HRE-irradiated measurements are compared.

Values of the ozone mixing ratio were plotted as a function of LST, as in Figure 5, where HRDI ozone mixing ratio data at 69 km altitude for May 6–30, 1992, at geographic locations with $3 < L \leq 4$ are shown. (In Figures 5–7, points drawn with crosses were observed during the HRE, points with open squares were measured before May 11, and those with diamonds after May 21.) The noise level is considerable, the standard deviation is estimated to be 0.07 ppmv on a daytime mean of 0.58 ppmv. Although the diurnal cycle is similar to the models of *Aikin and Smith* [1999] and *Allen et al.* [1984], there is no downward shift of the measurements during the HRE.

To increase the signal-to-noise ratio of the data, we averaged ozone values in 48 bins in LST. To avoid mixing undisturbed ozone values with those measured during the HRE, further reducing the strength and significance of the depletion signal, measurements made before May 11, after May 21, and from May 11 to May 21 (when the HRE flux is present) were separately averaged.

The diurnal cycle as observed by HRDI at 69 km in 30 min wide LST bins is shown in Figure 6. The error bars are drawn to illustrate one standard deviation of the mean of the data used to form the average. A maximum is present around noon with a minimum near 1500 LST. The rise of ozone prior to sunset is consistent with the model of *Aikin and Smith* [1999]. At other altitudes the measured LST dependence tracks the model calculations.

An examination of Figure 6 shows that data taken near the beginning of the yaw cycle are concentrated near and before local noon. During the HRE the observations are made between 0630–1030 and 1500–1830 LST. After the HRE has ended, data are observed in bands between 0530–0730 and 1100-1600 LST. It is therefore possible to compare ozone values at the same LST with different precipitating electron fluxes. The signature of an HRE-produced ozone depletion would be a consistent decrease in ozone when data at the same LST but with and without the electron irradiation are compared. In those three LST bands with such overlapping

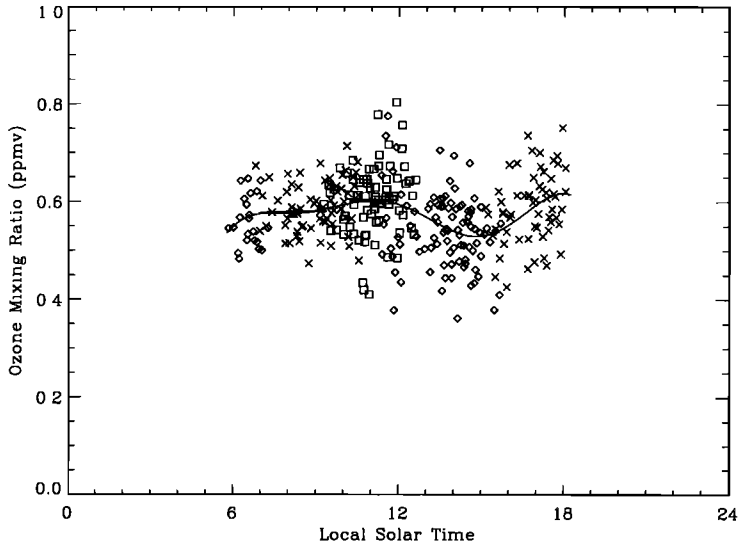

Figure 5. Ozone data at 69 km from the HRDI instrument, measured between May 6 and May 30, 1992 and with $3 < L \leq 4$ are shown. Data taken during the HRE (May 11–21) are labeled with a cross, data after May 21 are labeled with a diamond and before May 11 are labeled with a square. The solid line is a low-order Fourier fit to the data outlining the time dependence.

data, there is no consistent decrease in the ozone when the HRE is present.

6. Altitude Profiles

While there is no immediate indication for a decrease in ozone at 69 km during the May 1992 HRE, the four LST regions where ozone measurements during the May 1992 HRE overlap points taken before or after the HRE also have altitude profiles that can be compared. Consistent shifts in the ozone mixing ratio may be more apparent in those profiles. The GSFC-2D model prediction in Figure 4 shows an altitude profile that peaks between 65 and 70 km altitude and drops to zero at 55 and 90 km.

Immediately after sunrise (LSTs between 0630 and 0730) six profiles in the later part of the HRE overlap with 13 pro-

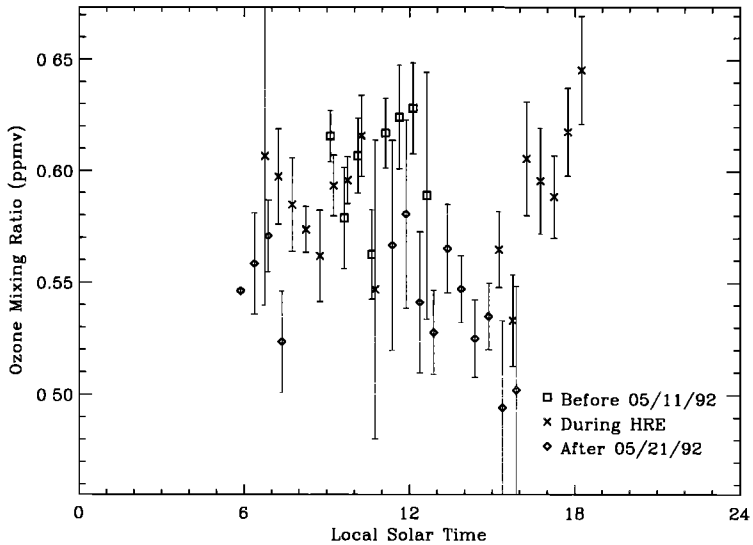

Figure 6. Ozone data at 69 km from the HRDI instrument, averaged over 30 min bins in LST. Data measured between May 6 and May 30, 1992, and with $3 < L \leq 4$ are shown. Separate averages of the data were done for three time periods. Averages of data taken during the May 1992 HRE (May 11–21) are labeled with a cross and are centered in the LST bin. Data measured before May 11 are labeled with a square and plotted 7.5 min before bin center. Data measured after May 21 are labeled with a diamond and plotted 7.5 min after bin center. This allows the symbols and error bars of each time period to be distinguished. The error bars show the standard deviation of the mean of the average in each LST bin.

files taken after the HRE. Owing to the rapid decay of the electron flux and the sensitivity of the ozone concentration to the electron-induced ionization in the GSFC-2D model, we expect to see a consistent decrease in the altitude profiles measured during the HRE. In Figure 7a we show two profiles, one an average of profiles during the HRE and the other an average of profiles taken after the HRE has ended, along with the standard deviation of the mean of each set. As the HRE-affected mixing ratios are always greater than the unaffected values (opposite to what was expected) and the error bars of the unaffected set do not encompass the average of the HRE-affected data, we conclude that a climatological decrease in mesospheric ozone may have occurred during the 4–6 days between the HRE and quiet conditions.

The next interval with overlapping measurements is midmorning (LSTs between 0900 and 1000), where the time-dependent chemistry model of *Aikin and Smith* [1999] predicts the greatest sensitivity to the electrons. At this point in the diurnal cycle, HO_x compounds have increased to a sufficient quantity to have an appreciable effect on the ozone.

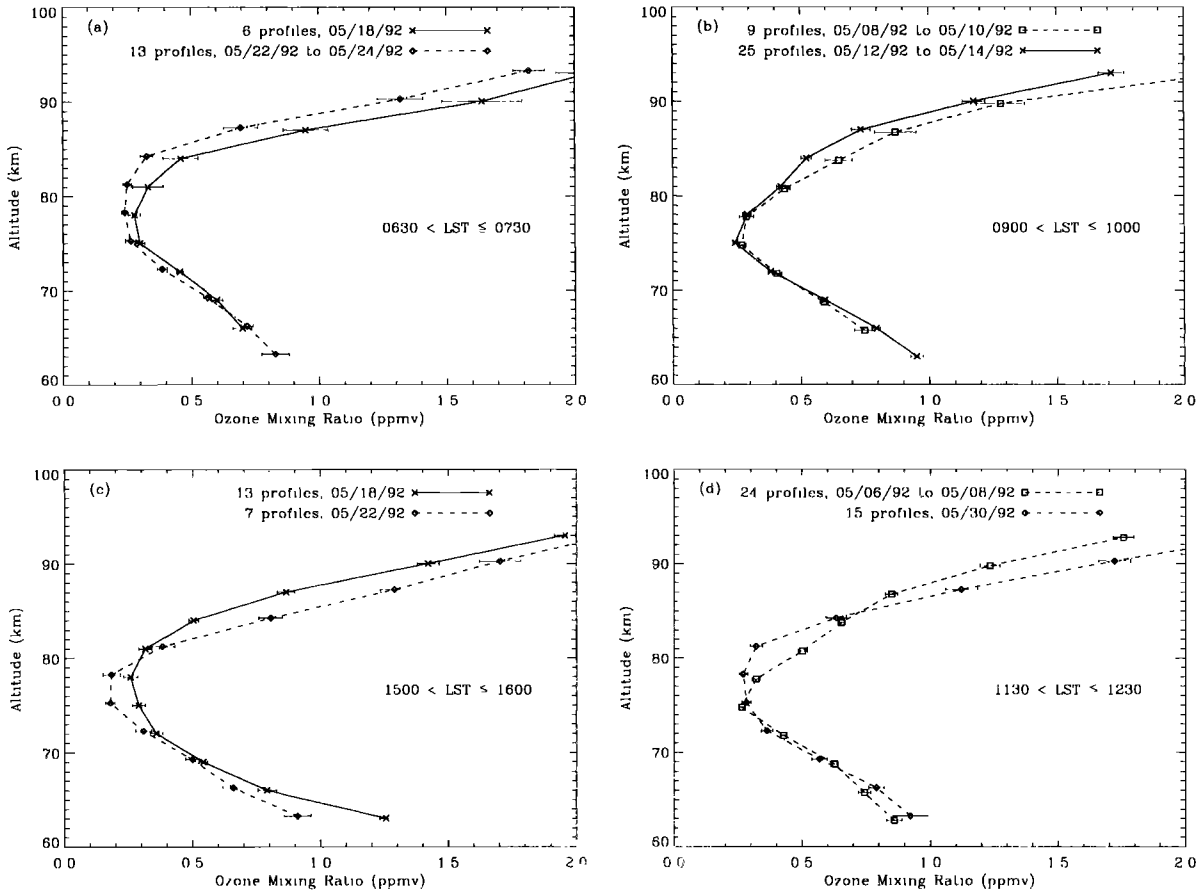

Figure 7. Altitude profiles of ozone data with overlapping LST values, measured between May 6 and May 30, 1992, and with $3 < L \leq 4$. Averages of profiles taken during the May 1992 highly relativistic electron event (HRE) are labeled with a cross, connected with a solid line, and plotted at the listed altitude. Averages of profiles measured before the HRE began are labeled with a square, connected with a dashed line, and shifted 0.5 km lower in altitude. Averages of profiles measured after the HRE had ended are labeled with a diamond, connected with a dot-dashed line, and shifted 0.5 km higher in altitude. The error bars represent the standard deviation of the mean of the average at each altitude. Individual plots are (a) ozone data with LST values between 0630 and 0730, comparing the average of six profiles measured on May 18 (during the HRE) with the average of 13 profiles measured after the HRE had ended (May 22–24); (b) ozone data with LST values between 0900 and 1000, comparing the average of 25 profiles measured between May 12 and 14 (during the HRE) with the average of nine profiles measured before the HRE began (May 8–10); (c) ozone data with LST values between 1500 and 1600, comparing the average of 13 profiles measured on May 18 (during the HRE) with the average of 7 profiles measured after the HRE had ended (May 22); (d) ozone data with LST values between 1130 and 1230, comparing the average of 24 profiles measured before the HRE (May 6–8) with the average of 15 profiles measured after the HRE had ended (May 30). There are no points measured during the HRE in Figure 7d, and any variations must be caused by other effects.

These points are a comparison of data taken across the onset of the HRE, when the precipitating fluxes increased by a factor of 100 at all energies in a short period of time (Figure 2a). Combining the rapid increase in electrons with the predicted sensitivity to that flux, this is the best opportunity for seeing the predicted effects. However, the measured values between 66 and 81 km are almost identical (Figure 7b). There may be a real decrease in the ozone at and above 85 km during the HRE, indicated by the separation of the measurements by more than the standard deviation of the HRE-affected ozone. At these altitudes the use of daily-averaged electron fluxes becomes less accurate, and the actual time dependence of the electron flux must be allowed for in the analysis.

The last comparison of HRE-irradiated with non-HRE material is for LST values between 1500 and 1600, predicted to be a region of low sensitivity to the electrons [*Aikin and Smith*, 1999]. In Figure 7c the ozone data have two altitude regions that must be discussed. Above 81 km the HRE-irradiated data are measurably below the points made 4 days later. Below 81 km it appears that the ozone mixing ratio during the HRE is larger than after. This may be due to the increasing concentration of water vapor in the mesosphere [*Chandra et al.*, 1997].

Finally, seasonal variations should be seen in Figure 7d, which shows two profiles which are averages of LST values between 1130 and 1230. Neither profile is directly affected by electrons, but they are separated by approximately 23 days. During those 3 weeks, increases in the H_2O concentration and solar irradiation should be reflected as differences between the two profiles. There is a tendency for ozone to decrease as a function of time below 85 km and increase above. Other studies of the seasonal variation of ozone showed that a decrease should be present at 80 km altitude during May, with good repeatability from year to year [*Thomas et al.*, 1984].

7. Effects of Water Vapor Changes on Ozone

While no HRE-induced decreases in ozone are seen, we do have consistent decreases in ozone below 81 km in the early morning, noon, and afternoon sectors as the month of May 1992 progressed. Given the climatological increase in mesospheric water vapor during the month of May [*Chandra et al.*, 1997], this decrease can be interpreted as a change in ozone brought about by the increasing water vapor content. Using the scaling relationship for daytime ozone at 70 km from Table 2 of *Allen et al.* [1984], we derive a relationship between changes in ozone and small changes in the electron flux and water vapor:

$$\frac{\Delta O_3}{O_3} = -\alpha\left(\frac{\varepsilon F_e}{J_5 + \varepsilon F_e} + \frac{\Delta[H_2O]}{[H_2O]}\right), \qquad (7)$$

where J_5 is the photolysis rate of H_2O and εF_e is the rate at which the HRE-induced ionizations create OH from H_2O [*Thomas et al.*, 1983]. The parameter α varies from 1/3 at 50 km to 1/2 at 70 and 1 at 80 km [*Allen et al.*, 1984]. The climatological variation of H_2O in the month of May at 80 km and 45°N is an increase by roughly 0.6 ppmv [*Chandra et al.*, 1997], roughly 16% of the total. Such a change is competitive with the HRE-induced changes and appears to be the cause of the ozone decreases observed in the HRDI data. Similar changes in mesospheric water vapor are reported in ground-based measurements at Table Mountain by *Nedoluha et al.* [1995]. Although this is a lower-latitude station, the increase in water vapor at 70 km is typically $\sim$ 20%, with a smaller increase in May 1992.

8. Summary and Conclusions

Mesospheric ozone data obtained from HRDI between altitudes of 66 and 81 km were examined for evidence of ozone depletions due to the precipitation of relativistic electrons in May 1992. Relative depletions of the order of the predicted values should have been seen when comparing ozone measurements made at those LSTs that were observed both with and without the HRE irradiation. Furthermore, the chemical models predict that the depletion amplitude should peak in the studied altitude region. Even if the precipitating electrons present in the May 1992 HRE caused significant ozone depletions in the mesosphere, the signal-to-noise ratio of the HRDI data, which had to be much less than a relative depletion of 20% to see the effect of a strong burst of flux, is not sufficient to measure the effect. It may be necessary to use ground-based measurements of ozone, water vapor, and electron-induced ionization of the same volume of the atmosphere to see the changes predicted by the models.

To reduce the scatter in the data, averages over 30 min LST bins were examined for ozone depletions correlated with altitude in those LST bins with measurements overlapping the onset and decay of the May 1992 HRE. At the altitudes examined here, depletions consistent with the available photochemical models were not found.

We have also found that it is not possible to average the ozone data over longer periods of time because of the sensitivity to the water vapor concentration. Variations in H_2O would cause UT-dependent changes in the LST ozone curves similar to those of the electron events. May is a time of rapid change in mesospheric water vapor [*Chandra et al.*, 1997; *Nedoluha et al.*, 1995]. Comparing the seasonal changes of ozone at 1500 LST [*Thomas et al.*, 1983] with the water vapor changes shows that changes in the ozone concentration are leading those in the water vapor, peaking just after the equinox, whereas the water vapor peaks near the solstice. This would indicate that the ozone concentration may be chemically reduced by the transported water vapor.

How can our conclusions be reconciled with the well-established ozone depletions in the stratosphere caused by solar proton events (SPEs)? The fluxes of protons connected with SPEs change relatively slowly over a time period of hours to a few days. Therefore the ozone depletion caused by an SPE also varies on these timescales and was observable for some events. Similarly, the daily-averaged fluxes of energetic electrons connected with HREs vary on timescales of days to weeks. However, the geographic coverages of the particle events do differ. Solar proton events are a po-

lar cap phenomenon, changing the composition over regions poleward of the $L = 5$ shell [*McPeters and Jackman*, 1985]. This means that a concave surface surrounds the depletion region and the depleted material is blown around the pole until it is restored to a normal concentration. By contrast, HREs are concentrated between L values of 3 and 4, with an interior region where the electron-induced changes are absent. Mesospheric winds would tend to dilute the chemical changes by moving material through the irradiation region, reducing the efficacy of the HRE electrons in changing the composition. We also note that both photochemical models assume that the HRE ion source is constant in time and space for periods longer than a day and areas large compared to the mixing region.

Although we have analyzed one of the most intense and longest-lasting HREs seen during the prime mission of UARS, we found no measurable effect on ozone in the middle mesosphere (this work) or the upper stratosphere and lower mesosphere [*Pesnell et al.*, 1999] of the Northern Hemisphere. However, given the more intense electron fluxes in the Southern Hemisphere, LST-resolved ozone observations in the south may yet reveal an HRE-related ozone depletion. In the absence of a consistent, measurable effect, the current results cast doubt on the long-term significance of the effect that highly relativistic electron events have on the overall ozone budget of ozone in the mesosphere and upper stratosphere. In particular, the sensitivity of mesospheric ozone to the water vapor content creates a large uncertainty in whether this effect is an important contribution to the long-term evolution of the mesosphere.

Acknowledgments. David P. Sletten assisted in the analysis and display of the UARS data. W.D.P is under contract at the Goddard Space Flight Center.

Janet G. Luhmann thanks Linwood B. Callis, George Reid, and another referee for their assistance in evaluating this paper.

References

Aikin, A. C., and H. J. P. Smith, Mesospheric constituent variations during electron precipitation events, *J. Geophys. Res.*, *104*, 26,457–26,471, 1999.

Allen, M., J. I. Lunine, and Y. L. Yung, The vertical distribution of ozone in the mesosphere and lower thermosphere, *J. Geophys. Res.*, *89*, 4841–4872, 1984.

Baker, D. N., P. R. Higbie, R. D. Belian, and E. W. Hones, Do Jovian electrons influence the terrestrial outer radiation zone?, *Geophys. Res. Lett.*, *6*, 531–534, 1979.

Baker, D. N., J. B. Blake, R. W. Klebesadel, and P. R. Higbie, Highly relativistic electrons in the Earth's outer magnetosphere, 1, Lifetimes and temporal history, *J. Geophys. Res.*, *91*, 4265–4276, 1986.

Baker, D. N., J. R. Blake, D. J. Gorney, P. R. Higbie, R. W. Klebesadel, and J. H. King, Highly relativistic magnetospheric electrons: A role in coupling to the middle atmosphere?, *Geophys. Res. Lett.*, *14*, 1027–1030, 1987.

Baker, D. N., R. A. Goldberg, F. A. Herrero, J. B. Blake, and L. B. Callis, Satellite and rocket studies of relativistic electrons and their influence on the middle atmosphere, *J. Atmos. Terr. Phys.*, *54*, 1619–1628, 1993.

Bojkov, R. D., *The Changing Ozone Layer*, World Meteorol. Org. and U. N. Environ. Programme, Geneva, 1995.

Brasseur, G., and S. Solomon, *Aeronomy of the Middle Atmosphere*, 2nd ed., Reidel, Norwell, Mass., 1986.

Burrage, M. D., et al., Validation of mesosphere and lower thermosphere winds from the high-resolution Doppler imager on UARS, *J. Geophys. Res.*, *101*, 10,365–10,392, 1996.

Chandra, S., C. H. Jackman, E. L. Fleming, and J. M. Russell III, The seasonal and long term changes in mesospheric water vapor, *Geophys. Res. Let.*, *24*, 639–642, 1997.

Fleming, E. L., S. Chandra, C. H. Jackman, D. B. Considine, and A. R. Douglass, The middle atmospheric response to short and long term solar UV variations: Analysis of observations and 2D model results, *J. Atmos. Terr. Phys.*, *57*, 333–365, 1995.

Gaines, E. E., D. L. Chenette, W. L. Imhof, C. H. Jackman, and J. D. Winningham, Relativistic electron fluxes in May 1992 and their effect on the middle atmosphere, *J. Geophys. Res.*, *100*, 1027–1033, 1995.

Goldberg, R. A., An experimental search for causal mechanisms in Sun/weather-climatic relationships, in *Solar-Terrestrial Influences on Weather and Climate*, edited by B. M. McCormac and T. A. Seliga, pp. 161–173, Reidel, Norwell, Mass., 1979.

Goldberg, R. A., C. H. Jackman, J. R. Barcus, and F. Sørass, Nighttime auroral energy deposition in the middle atmosphere, *J. Geophys. Res.*, *89*, 5581–5590, 1984.

Goldberg, R. A., D. N. Baker, F. A. Herrero, S. P. McCarthy, P. A. Twigg, C. L. Croskey, and L. C. Hale, Energy deposition and middle atmosphere electrodynamic response to a highly relativistic electron precipitation event, *J. Geophys. Res.*, *99*, 21,071–21,081, 1994.

Goldberg, R. A., C. H. Jackman, D. N. Baker, and F. A. Herrero, Changes in the concentration of mesospheric O_3 and OH during a highly relativistic electron precipitation event, in *The Upper Mesosphere and Lower Thermosphere: A Review of Experiment and Theory*, *Geophys. Monogr. Ser.*, vol. 87,edited by R. M. Johnson and T. L. Killeen, pp. 215–223, AGU, Washington, D.C., 1995a.

Goldberg, R. A., D. N. Baker, F. A. Herrero, C. H. Jackman, S. Kanekal, and P. A. Twigg, Mesospheric heating during highly relativistic electron precipitation events, *J. Geomagn. Geoelectr.*, *47*, 1237–1247, 1995b.

Hays, P. B., V. J. Abreu, M. E. Dobbs, D. A. Gell, H. J. Grassl, and W. R. Skinner, The high-resolution Doppler imager on the Upper Atmosphere Research Satellite, *J. Geophys. Res.*, *98*, 10,713–10,723, 1993.

Herrero, F. A., D. N. Baker, and R. A. Goldberg, Rocket measurements of relativistic electrons: New features in fluxes, spectra and pitch angle distributions, *Geophys. Res. Lett.*, *18*, 1481–1484, 1991.

Imhof, W. L., and E. E. Gaines, Inputs to the atmosphere from relativistic electrons, *J. Geophys. Res.*, *98*, 13,575–13,580, 1993.

Imhof, W. L., H. D. Voss, J. Mobilia, D. W. Datlowe, J. P. McGlennon, and D. N. Baker, Relativistic electron enhancement events: Simultaneous measurements from synchronous and low altitude satellites, *Geophys. Res. Lett.*, *18*, 397–400, 1991.

Jackman, C. H., Effects of energetic particles on minor constituents of the middle atmosphere, *J. Geomagn. Geoelectr.*, *43*, Suppl., 637–640, 1991.

Jackman, C. H., A. R. Douglass, R. B. Rood, R. D. McPeters, and P. E. Meade, Effects of solar proton events on the middle atmosphere during the past two solar cycles as computed using a two-dimensional model, *J. Geophys. Res.*, *95*, 7417–7428, 1990.

Jackman, C. H., E. L. Fleming, S. Chandra, D. B. Considine, and J. E. Rosenfield, Past, present, and future modeled ozone trends with comparisons to observed trends, *J. Geophys. Res.*, *101*, 28,753–28,767, 1996.

Lauter, E. A., and R. Knuth, Precipitation of high energy particles into the upper atmosphere at medium latitudes after magnetic storms, *J. Atmos. Terr. Phys.*, *29*, 411–417, 1967.

McPeters, R. D., and C. H. Jackman, The response of ozone to solar proton events during solar cycle 21: The observations, *J. Geophys. Res.*, *90*, 7945–7954, 1985.

Nedoluha, G. E., R. M. Bevilacqua, R. M. Gomez, D. L. Thacker, W. B. Williams, and T. A. Pauls, Ground-based measurements of water vapor in the middle atmosphere, *J. Geophys. Res.*, *100*, 2927–2939, 1995.

Pesnell, W. D., R. A. Goldberg, C. H. Jackman, D. L. Chenette, and E. E. Gaines, A search of UARS data for ozone depletions caused by the highly relativistic electron precipitation events of May 1992, *J. Geophys. Res.*, *104*, 165–175, 1999.

Potemra, T. A., and A. J. Zmuda, Precipitating energetic electrons as an ionization source in the midlatitude nighttime *D* region, *J. Geophys. Res.*, *75*, 7161–7167, 1970.

Rostoker, G., S. Skone, and D. N. Baker, On the origin of relativistic electrons in the magnetosphere associated with some geomagnetic storms, *Geophys. Res. Lett.*, *25*, 3701-3704, 1998.

Solomon, S., D. W. Rusch, J.-C. Gerard, G. C. Reid, and P. J. Crutzen, The effect of particle precipitation events on the neutral and ion chemistry of the middle atmosphere, 2, Odd hydrogen, *Planet. Space Sci.*, *29*, 885–892, 1981.

Solomon, S., G. C. Reid, D. W. Rusch, and R. J. Thomas, Mesospheric ozone depletion during the solar proton event of July 13, 1982, 2, Comparison between theory and measurements, *Geophys. Res. Lett.*, *10*, 257–260, 1983.

Spjeldvik, W. N., and R. M. Thorne, The cause of storm after effects in the middle latitude *D*-region, *J. Atmos. Terr. Phys.*, *37*, 777-795, 1975.

Thomas, R. J., C. A. Barth, G. J. Rottman, D. W. Rusch, G. H. Mount, G. M. Laurence, R. W. Sanders, G. E. Thomas, and L. E. Clemens, Mesospheric ozone depletion during the solar proton event of July 13, 1982, 1, Measurement, *Geophys. Res. Lett.*, *10*, 253–255, 1983.

Thomas, R. J., C. A. Barth, and S. Solomon, Seasonal variation of ozone in the upper mesosphere and gravity waves, *Geophys. Res. Lett.*, *11*, 673–676, 1984.

Thorne, R. M., Energetic radiation belt electron precipitation: A natural depletion mechanism for stratospheric ozone, *Science*, *195*, 187-189, 1977.

Vampola, A. L., and D. J. Gorney, Electron energy deposition in the middle atmosphere, *J. Geophys. Res.*, *88*, 6267–6274, 1983.

Walt, M., *Introduction to Geomagnetically Trapped Radiation*, pp. 44–50, Cambridge Univ. Press, New York, 1994.

Winningham, J. D., et al., The UARS particle environment monitor, *J. Geophys. Res.*, *98*, 10,649–10,666, 1993.

D. L. Chenette and E. E. Gaines, Space Physics Department, Lockheed Martin Advanced Technology Center, O/L9-42, Building 255, 3251 Hanover Street, Palo Alto, CA 94304. (Chenette@spasci.com; Gaines@spasci.com)

R. A. Goldberg, Laboratory for Extraterrestrial Physics, Code 690, NASA Goddard Space Flight Center, Greenbelt, MD 20771. (Richard.A.Goldberg.2@gsfc.nasa.gov)

C. H. Jackman, Laboratory for Atmospheres, Code 916, NASA Goddard Space Flight Center, Greenbelt, MD 20771. (Charles.Jackman@gsfc.nasa.gov)

W. D. Pesnell, Nomad Research, Inc., 2804 Nomad Court, Bowie, MD 20716. (Pesnell@NomadResearch.com)

(Received March 15, 2000; revised May 19, 2000; accepted May 25, 2000)